Thermochimica Acta 517 (2011) 40–44

Contents lists available at ScienceDirect

Thermochimica Acta

journal homepage: www.elsevier.com/locate/tca

Kinetic and thermodynamic study of the reaction catalyzed by glucose-6-phosphate dehydrogenase with nicotinamide adenine dinucleotide

Julia S. Martín del Campo, Rodrigo Patiño*

Departamento de Física Aplicada, Centro de Investigación y de Estudios Avanzados – Unidad Mérida, Carretera antigua a Progreso Km. 6, A.P. 73 Cordemex, 97310, Mérida, Yucatán, Mexico

ARTICLE INFO

Article history:
Received 11 October 2010
Received in revised form 11 January 2011
Accepted 20 January 2011
Available online 25 February 2011

Keywords:
Equilibrium constant
Gibbs energy
Enzymatic kinetics
Leuconostoc mesenteroides
β-Nicotinamide adenine dinucleotide
6-Phospho-D-glucono-1,5-lactone

ABSTRACT

The enzyme glucose-6-phosphate dehydrogenase (G6PD, EC 1.1.1.49) from *Leuconostoc mesenteroides* has a dual coenzyme specificity with oxidized nicotinamide adenine dinucleotide (NAD_{ox}) and oxidized nicotinamide adenine dinucleotide phosphate as electron acceptors. The G6PD coenzyme selection is determined by the metabolic cellular prevailing conditions. In this study a kinetic and thermodynamic analysis is presented for the reaction catalyzed by G6PD from *L. mesenteroides* with NAD_{ox} as coenzyme in phosphate buffer. For this work, an *in situ* spectrophotometric technique was employed based on the detection of one product of the reaction. Substrate and coenzyme concentrations as well as temperature and pH effects were evaluated. The apparent equilibrium constant, the Michaelis constant, and the turnover number were determined as a function of each experimental condition. The standard transformed Gibbs energy of reaction was determined from equilibrium constants at different initial conditions. For the product 6-phospho-D-glucono-1,5-lactone, a value of the standard Gibbs energy of formation is proposed, $\Delta_f G^\circ = -1784 \pm 5\ kJ\ mol^{-1}$.

1. Introduction

The enzyme glucose-6-phosphate dehydrogenase (G6PD; EC 1.1.1.49) is the first enzyme of the pentose phosphate pathway, an alternative path for glucose metabolism in cells. The generation of reduced β-nicotinamide adenine dinucleotide (NAD_{red}) and of ribose residues is the principal function of this path. The G6PD from the bacteria *Leuconostoc mesenteroides* [1] is a 109,603 Da two-subunit enzyme that catalyzes the oxidation of glucose-6-phosphate (G6P) to 6-phospho-D-glucono-1,5-lactone (6PDGL). This enzyme has dual coenzyme specificity: it can reduce both NAD^+ (NAD_{ox}) and $NADP^+$ ($NADP_{ox}$), with a hydrogen atom addition (Fig. 1).

The election between NAD_{ox} and $NADP_{ox}$ is controlled by cellular metabolic conditions. In *L. mesenteroides*, these reduced coenzymes take part in different pathways: $NADP_{red}$ is used in fatty acids biosynthesis while NAD_{red} is used in heterolactic fermentation [2]. By using site-directed mutagenesis, the catalytic mechanism of G6PD has been elucidated. The reported results support a mechanism in which the residue His-240 is hydrogen bonded to the residue Asp-177, forming a catalytic dyad. Then, the N∈2 of the His-240 is poised to act as a general base by abstracting a proton from the C1–OH of the G6P, allowing a transfer of the C1–hydride to the C4 position of the nicotinamide ring of the NAD_{ox} or of the $NADP_{ox}$ [3]. Therefore, the His-240 plays an important role in the G6PD activity and the protonation of this $pK_a = 6.4$ residue diminishes the enzymatic activity [1].

The mechanism of thermal inactivation for G6PD from *Saccharomyces cerevisiae* has been studied and it was found that at temperatures higher than $T = 308$ K, the half-life time values are very low and the enzyme is denatured rapidly [4]. Thermodynamic and kinetic studies of the synthesis and activity of G6PD from *S. cerevisiae* have been reported [5], however similar results were not found for G6PD from *L. mesenteroides.* Although there are some kinetic and thermodynamic data for the G6PD activity with $NADP_{ox}$, the experimental work is old and not detailed, and the results are difficult to compare systematically [6,7].

In this work, the G6PD activity with NAD_{ox} in phosphate buffer was studied using an *in situ* spectrophotometric technique. The kinetics analysis was performed in base of the Michaelis–Menten model: the Michaelis constant (K_M) and the turnover number (k_{cat}) were obtained at different temperature and pH values. The standard transformed Gibbs energy of reaction was obtained by employing

Abbreviations: G6P, glucose-6-phosphate; G6PD, glucose-6-phosphate dehydrogenase; $NAD_{ox} = NAD^+$, oxidized β-nicotinamide adenine dinucleotide; $NAD_{red} = NADH$, reduced β-nicotinamide adenine dinucleotide; $NADP_{ox} = NADP^+$, oxidized β-nicotinamide adenine dinucleotide phosphate; $NADP_{red} = NADPH$, reduced β-nicotinamide adenine dinucleotide phosphate; 6PDGL, 6-phospho-D-glucono-1,5-lactone.

* Corresponding author. Tel.: +52 999 9429438; fax: +52 999 9812917.
E-mail address: rtarkus@mda.cinvestav.mx (R. Patiño).

0040-6031/$ – see front matter © 2011 Elsevier B.V. All rights reserved.
doi:10.1016/j.tca.2011.01.030

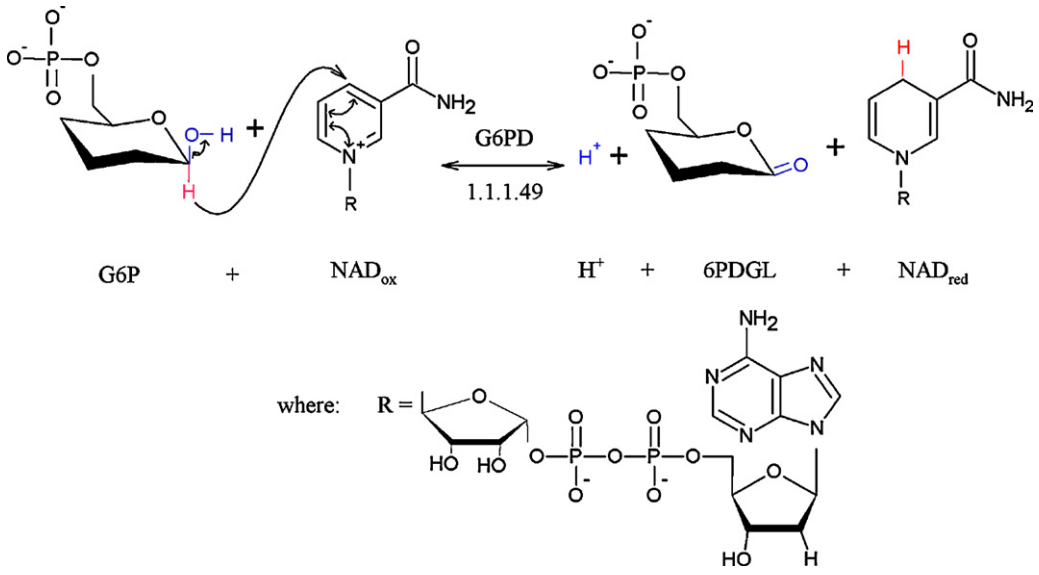

Fig. 1. Reaction catalyzed by G6PD with NADox.

the recommended specific equations for biochemical reactions [8]. Based on this methodology, the standard Gibbs energy of formation of the product 6PDGL was calculated.

2. Experimental methods

2.1. Reaction solutions

The reaction system consisted of molar solutions of G6P and NAD_{ox} in (50.0 ± 0.1) mM phosphate buffer. The phosphate buffer was prepared in deionized water with monobasic potassium phosphate (Química Meyer, KH_2PO_4, purity 0.998) and dibasic potassium phosphate (Química Meyer, K_2HPO_4, purity 0.997). The relative concentrations were calculated from the Henderson–Hasselbach equation with $pK_a = 6.89$ [9]. The pH value of the buffer was adjusted with HCl or NaOH, both at 1.0 M of concentration, and verified with a potentiometer (SensIon 3; ±0.01). The G6PD enzyme from *L. mesenteroides* was acquired as lyophilized powder (Sigma, 640 units (mg protein)$^{-1}$) and was dissolved in pH 7.0, 50 mM phosphate buffer. As substrate, the crystallized D-glucose 6-phosphate sodium salt (Sigma, $C_6H_{12}NaO_9P$, purity 0.98) and the coenzyme β-nicotinamide adenine dinucleotide sodium salt (Sigma, $C_{21}H_{26}N_7NaO_{14}P_2$, purity 0.95, from *Saccharomyces cerevisiae*) were used. Stock solutions [NAD_{ox}] = (75.0 ± 0.1) mM and [G6P] = (10.0 ± 0.1) mM were prepared in the 50 mM phosphate buffer at the corresponding pH value. For each experiment, these solutions were diluted with the same 50 mM phosphate buffer to reach the desired initial substrate concentrations. In all cases, the final enzyme concentration was 0.2 U mL^{-1}.

2.2. Reactor and probe mounting

The reactor (Fig. 2) consisted of a 50 mL three-neck round-bottom flask, submerged in a circulating bath (Isotemp 3016, Fisher) at the work temperature (±0.05 K). In the flask, the reaction mixture was deposited in the next order: first the G6P solution, then the NAD_{ox} solution and, finally, the enzyme solution to start the reaction. In order to maintain the homogeneity in temperature and composition during the reaction, a glass two-bladed propeller was used and rotated at 100 rpm by a mechanic mixer through a flexible stirrer shaft. The evolution of the reaction was followed in real time, monitoring the NAD_{red} product formation with a maximum of absorption at 340 nm of wavelength, through an optical probe connected to a spectrophotometer (EPP2000, StellarNet) with 0.20 or 2.0 cm of cell length. The length of the cell was chosen in order to get absorbance values between 0.1 and 1.0. The control of the spectrometer and the automatic data compilations were done through a PC interface with the corresponding SpectraWiz software. The reaction time varied from 1000 to 3000 s as a function of the substrates concentrations, pH values and temperature; however, in all experiments, 200 episodes were recorded and the duration between each episode was a function of the monitoring time during the reaction.

2.3. Different temperature and pH experiments

All experiments were done in duplicate. Different substrate G6P:NAD_{ox} concentration relations: (0.10:1.0, 1.0:0.10, 1.0:1.0, 1.0:7.5 and 7.5:1.0) mM were analyzed at different values of pH and temperature. At pH 7.00 ± 0.01, a series of T/K = (292.15, 298.15, 304.15, 310.5 and 316.15) was performed. The pH buffer variation was studied at (298.15 ± 0.05) K with pH 5.4, 6.2, 7.0, 7.8 or 8.6.

3. Results

The reaction initial rates were based on the time evolution of the optical absorbance (A) of the product NAD_{red} formed during

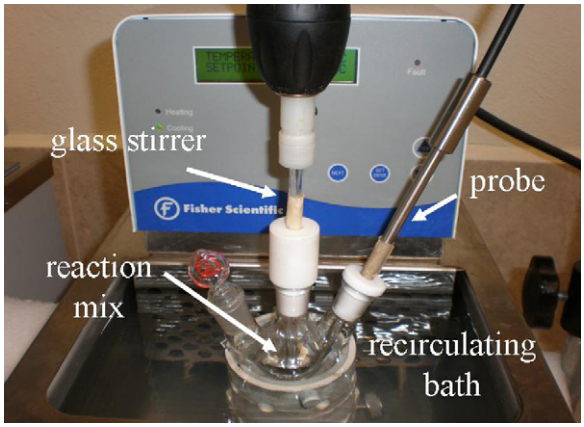

Fig. 2. Experimental setup (the lid was retired for a better description).

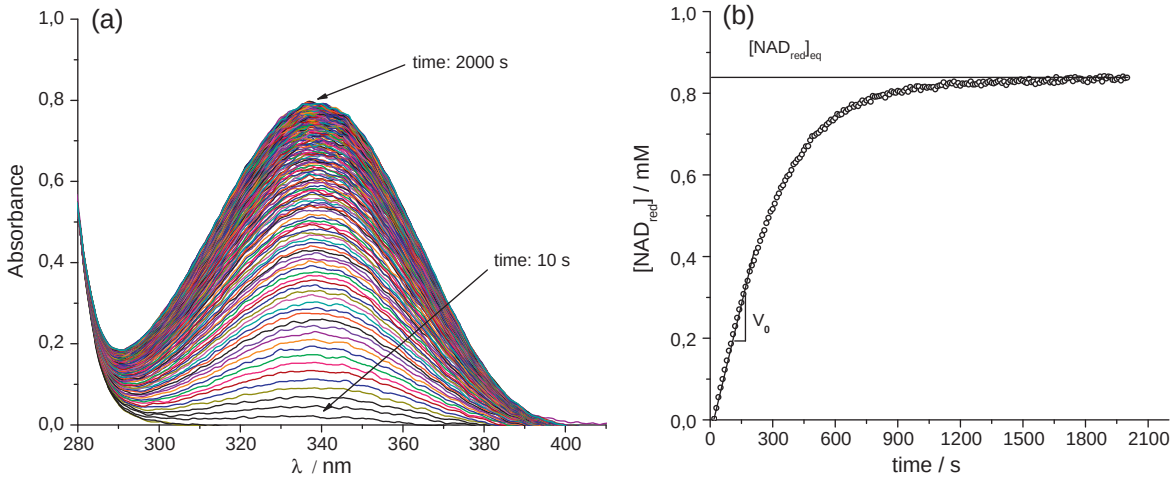

Fig. 3. (a) Time evolution of the UV-absorption spectra during the enzymatic oxidation by G6PD. The signal around 340 nm is from the product NAD_{red}. (b) NAD_{red} concentration evolution with time, obtained with the Lambert–Beer law. The experimental conditions were $T = 298.15$ K and 50 mM phosphate buffer at pH 7.00, with initial concentrations $[G6P]_0 = 7.5$ mM, $[NAD_{ox}]_0 = 1.0$ mM and 0.2 U mL^{-1} of enzyme concentration.

the process, a typical example is shown in Fig. 3a. The reaction progress was followed at $\lambda_{max}(NAD_{red}) = 340$ nm of the maximal wavelength using the Lambert–Beer law, $A = (\varepsilon, \text{mM}^{-1}\,\text{cm}^{-1})(l, \text{cm})(c, \text{mM})$, where c is the NAD_{red} concentration ($[NAD_{red}]$) at any time, l is the optical path length, and the extinction coefficient for NAD_{red} is $\varepsilon = 6.22\ \text{mM}^{-1}\,\text{cm}^{-1}$. Fig. 3b represents a characteristic curve of the reaction progress for the data in Fig. 3a. The initial rate (V_0, mM s^{-1} = d$[NAD_{red}]$/dt) corresponds to the slope of the linear tendency obtained at the beginning of the reaction; in all the cases, the linear coefficient of determination was $R^2 \geq 0.95$. A mean value of V_0 was computed from the duplicates with the corresponding standard deviation as the uncertainty. The equilibrium concentration of the products, $[NAD_{red}]_{eq} = [6PDGL]_{eq}$, was calculated as an average of the concentration in the region of the curve where the slope is zero. In order to verify that a true equilibrium was achieved, a number of preliminary experiments at different enzyme concentrations were performed with the same substrate and coenzyme concentrations: the same equilibrium concentration was obtained independently of the catalyst concentration. Supplementary data shows a Table S1 with $[NAD_{red}]_{eq}$ values at different enzyme and substrate concentrations, and two tables with the mean values of V_0 and $[NAD_{red}]_{eq}$ at 45 different experimental conditions, as a function of the pH (Table S2) and the temperature (Table S3).

4. Discussion

4.1. Kinetic constants

The G6PD kinetic activity with G6P and NAD_{ox} obeys the Michaelis–Menten law with an independent binding of substrates [4]. In this work, the K_M and V_{max} constants from the Michaelis–Menten model were obtained with the Lineweaver–Burk (L–B) and the Eadie–Hofstee (E–H) equations using weighted linear fits. The K_M values were computed twice considering the G6P or the NAD_{ox} as substrate. From the obtained V_{max} constants, the k_{cat} was calculated for each experimental condition considering two active sites for every enzyme; the values are presented in Table 1. The G6P has a value of p$K_a = 5.99$ at the ionic strength $I = 0.10$ M for the following equilibrium that is presented in the pH range of this study [9]:

$$G6P^{-1} = G6P^{-2} + H^{+} \quad (1)$$

Fig. 4 represents the distribution with the pH of the molar fraction for these G6P species and for the His-240 residue (p$K_a = 6.4$) [1]. At pH ≥ 7 the $G6P^{-2}$ is the principal pseudoisomer of G6P in solution and the His-240 is almost totally deprotonated which allows a better enzyme–substrate interaction, based on the mechanism described where His-240 acts as general base abstracting a hydro-

Table 1
Kinetic parameters of the reaction as (a) pH functions at $T = 298.15$ K, and as (b) temperature functions at pH 7.00, both with 0.2 U mL^{-1} of enzyme concentration in 50 mM phosphate buffer ($I = 0.1$ M).

	K_M (mM)×10^{-2}				V_{max} (mM s^{-1})×10^{-3}		k_{cat} (min^{-1})×10^{3}	
	G6P		NAD_{ox}					
	L–B[a]	E–H[b]	L–B	E–H	L–B	E–H	L–B	E–H
(a) pH								
5.40	13 ± 8	22 ± 4	19 ± 4	19 ± 3	0.49 ± 0.05	0.49 ± 0.04	5.1 ± 0.5	5.1 ± 0.4
6.20	38 ± 5	40 ± 1	22 ± 3	48 ± 1	1.49 ± 0.08	1.60 ± 0.03	15.7 ± 0.9	16.9 ± 0.3
7.00	47 ± 1	47 ± 1	39 ± 6	40 ± 6	2.37 ± 0.33	2.40 ± 0.26	25.0 ± 3.5	25.2 ± 2.7
7.80	61 ± 8	60 ± 2	38 ± 4	38 ± 1	2.70 ± 0.10	2.70 ± 0.09	28.4 ± 1.1	28.4 ± 1.0
8.60	69 ± 7	88 ± 2	46 ± 4	46 ± 1	3.23 ± 0.23	3.42 ± 0.08	34.0 ± 2.4	36.0 ± 0.9
(b) T/K								
292.15	32 ± 3	33 ± 3	43 ± 7	43 ± 2	2.17 ± 0.08	2.07 ± 0.17	21.7 ± 2.0	21.8 ± 1.7
298.15	47 ± 1	47 ± 1	39 ± 6	40 ± 6	2.27 ± 0.33	2.40 ± 0.26	25.0 ± 3.5	25.2 ± 2.7
304.15	58 ± 5	65 ± 1	39 ± 7	52 ± 3	2.68 ± 0.04	2.83 ± 0.03	29.4 ± 0.5	29.8 ± 0.3
310.15	87 ± 4	89 ± 0	61 ± 6	66 ± 1	4.03 ± 0.04	4.25 ± 0.01	44.6 ± 0.4	44.8 ± 0.1
316.15	57 ± 11	59 ± 9	66 ± 11	68 ± 10	4.26 ± 0.70	4.11 ± 0.76	42.1 ± 10.2	43.3 ± 8.0

[a] Data from the Lineweaver–Burk method analysis.
[b] Data from the Eadie–Hofstee method analysis.

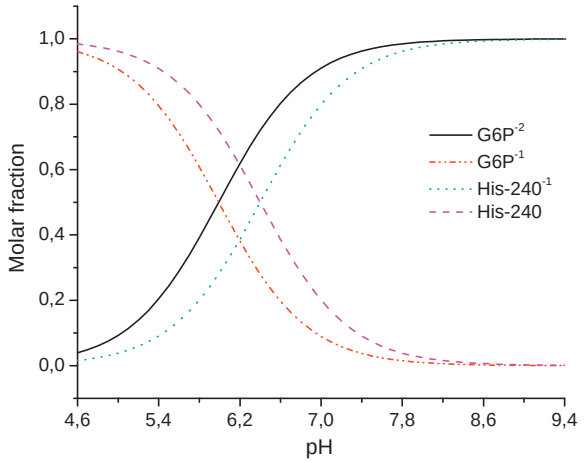

Fig. 4. Molar fraction as a function of the pH for the pseudisomer species of G6P ($pK_a = 5.99$ at $I = 0.1$ M), and of the His-240 residue ($pK_a = 6.4$).

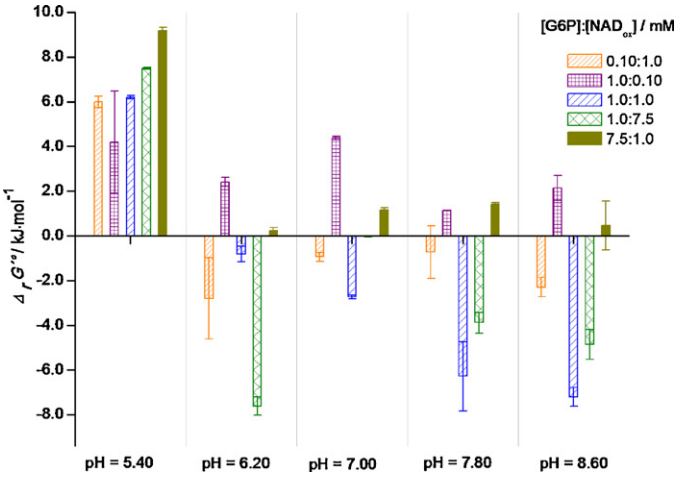

Fig. 5. Standard transformed Gibbs energy of reaction $\Delta_r G'^{\circ}$ as function of the pH and the relative G6P:NAD_{ox} concentrations, at $T = 298.15$ K in 50 mM phosphate buffer. The uncertainty bars represent the propagated error from K' values.

gen from the G6P [3]. Table 1(a) shows how the k_{cat} values increase with pH, principally in the range from pH 5.4 to pH 7.0. This could be explained since $G6P^{-2}$ species concentration increases; in addition, the His-240 residue of G6PD with pK_a of 6.4 is deprotonated and, as consequence, the number of functional active sites increases [1].

As temperature was increased from 292.15 K to 310.15 K, k_{cat} values increased, and at $T = 316.15$ K the enzyme thermal instability is remarkable [4,5], provoking an increasing in the uncertainty of the measurement, as seen in Table 1(b). From k_{cat} values, which are zero order rate constants, the activation energy, E_a, was calculated with the Arrhenius equation: in the range from 292.15 K to 310.15 K, $E_a = (46 \pm 13)$ kJ mol^{-1} at pH 7.0 and $I = 0.1$ M. Some values for K_M and k_{cat} are reported in the literature for the same reaction with G6PD [10–12], however, the results in this work can not be compared since the Hofmeister effects are important [13,14]. These effects are related with unlike activities of the same enzyme with different buffer species, even at the same pH.

4.2. Thermodynamic parameters of reaction

From NAD_{red} equilibrium concentrations, the apparent equilibrium constants of reaction K' were calculated with Eq. (2):

$$K' = \frac{[NAD_{red}]_{eq}[6PDGL]_{eq}}{[G6P]_{eq}[NAD_{ox}]_{eq}} = \frac{[NAD_{red}]_{eq}^2}{\left([G6P]_0 - [NAD_{red}]_{eq}\right)\left([NAD_{ox}]_0 - [NAD_{red}]_{eq}\right)} \quad (2)$$

The K' values for this reaction have been reported by Brink [15] in 0.13 M phosphate buffer, at pH 7 and $T = 294.15$ K: $K' = 2.9$ ($[G6P]_0 = 0.133$ mM, $[NAD_{ox}]_0 = 0.0404$ mM) and $K' = 3.3$ ($[G6P]_0 = 0.0667$ mM, $[NAD_{ox}]_0 = 0.0394$ mM). These reported values and the K' values in this work show the influence of the reactants initial concentrations. However, since the effect of the ionic strength is also remarkable on the K' values, it is not correct to compare the values by Brink with those in this work due to the different experimental solution concentrations.

From the K' values, the standard transformed Gibbs energy of reaction $\Delta_r G'^{\circ}$ was obtained with Eq. (3):

$$\frac{\Delta_r G'^0}{R} = -T \ln K' \quad (3)$$

In Fig. 5, the effect of the pH and the relative concentration G6P:NAD_{ox} on $\Delta_r G'^{\circ}$ values is shown at $T = 298.15$ K and $I = 0.1$ M. At pH 5.4, it is remarkable the effect on the positive values of the transformed Gibbs energy of reaction and it can be explained by the abundance of $G6P^{-1}$ species (Fig. 4). At pH ≥6.2, it is possible to observe the effect of relative substrate:coenzyme concentration. In general, when $[G6P]_0 < [NAD_{ox}]_0$, the biochemical reaction is thermodynamically favored; the opposite situation occurs when $[G6P]_0 > [NAD_{ox}]_0$. For $[G6P]_0 = [NAD_{ox}]_0$, the increase of pH favors thermodynamically the reaction.

The $\Delta_r G'^{\circ}$ values obtained as function of the temperature do not show a good correlation, for this reason the computation of standard transformed enthalpy of reaction could not be possible. To obtain an acceptable value of this thermodynamic parameter, it should be necessary a calorimetric study [16].

4.3. Standard Gibbs energy of formation of 6PDGL

To calculate the standard Gibbs energy of formation of 6PDGL (pH 7.0, $p = 1$ bar and $I = 0$ M), the methodology developed by Alberty was followed [8,9]. For each species j of the reaction, the empiric Eq. (4) was employed:

$$\frac{\Delta_f G_j^0(I=0)}{R} = \frac{\Delta_f G'^0_j}{R} - N_H(j)\left(\frac{T}{K}\right)\ln 10\,\mathrm{pH} + \frac{(\alpha/M^{-1/2})(T/K)(z_j^2 - N_H(j))(I^{1/2}/M^{1/2})}{1 + (1.6/M^{-1/2})(I^{1/2}/M^{1/2})} \quad (4)$$

where z_j is the charge and the term $N_H(j)$ is the number of hydrogen bounded atoms; the α parameter is reported and it is a function of temperature. The conversion by employing this equation generates an error of ±0.01 kJ mol^{-1}.

To obtain the transformed standard Gibbs energy of formation of G6P, $\Delta_f G'^{\circ}$(G6P), for each pH value, the equilibrium of pseudoisomer groups was considered and calculated through the binding polynomial equation that considers the dissociation constant of G6P as function of both I and pH. In summary, to obtain the $\Delta_f G^{\circ}$ of 6PDGL the following operations were followed: (i) the experimental $\Delta_r G'^{\circ}$ values were calculated from apparent equilibrium constants (Eq. (3)); (ii) the values of the standard Gibbs energy of formation, $\Delta_f G^{\circ}$, of $G6P^{-2}$ (−1763.94 kJ mol^{-1} and $pK_a = 5.99$ at $I = 0.10$ M), NAD_{ox} (0 kJ mol^{-1}), NAD_{red} (22.65 kJ mol^{-1}) and H^+ (0 kJ mol^{-1}) were transformed at the $\Delta_f G'^{\circ}$(j) for the corresponding experimental conditions; (iii) the calculation of $\Delta_f G'^{\circ}$ for 6PDGL by subtraction of $\Delta_f G'^{\circ}$(j) from $\Delta_r G'^{\circ}$; (iv) finally, the obtained $\Delta_f G'^{\circ}$ values of 6PDGL were transformed by Eq. (4) to the corresponding $\Delta_f G^{\circ}$, considering a −2 charge in the studied range of pH.

Table 2
Standard Gibbs energy of formation of 6-phospho-D-glucono-1,5-lactone (6PDGL) at different values of pH and temperature. The mean value corresponds to the average of the eight reported values.

pH at T = 298.15 K	$\Delta_f G^\circ$ (6PDGL) (kJ mol^{-1})	T/K at pH = 7.00	$\Delta_f G^\circ$ (6PDGL) (kJ mol^{-1})
5.40	−1781 ± 2	292.15	−1785 ± 2
6.20	−1787 ± 2	298.15	−1784 ± 1
7.00	−1784 ± 1	304.15	−1783 ± 1
7.80	−1786 ± 2	310.15	−1785 ± 1
8.60	−1786 ± 2	Mean value: $\Delta_f G^\circ$ (6PDGL) = −(1784 ± 5) kJ mol^{-1}	

In the range of temperature from 292.15 K to 310.15 K and in the range of pH from 5.4 to 8.6, it was found that the average standard Gibbs energy of formation of 6PDGL is $\Delta_f G^\circ$(G6PDL) = −(1784 ± 5) kJ mol^{-1} (Table 2).

The explanation to consider this −2 charge for 6PDGL is given as follows: since the pK_a value was not found in the literature for the product 6PDGL, the transformed Gibbs energy of formation of 6PDGL as pH function keeps a linear relation that is described by the Eq. (5) [9]:

$$\bar{N}_H = \frac{1}{(T/K)\ln 10}\left(\frac{\partial(\Delta_f G'^0/R)}{\partial pH}\right)_{T,p,n_i} \quad (5)$$

where $\bar{N}_H$ is the average number of hydrogen atoms bounded by the reactant. If temperature, pressure and species number are constant, it is possible to obtain easily the integrated form of Eq. (5) and, by a linear regression of $\Delta_f G'^\circ$ (6PDGL) *versus* pH, the slope obtained corresponds to $\bar{N}_H = 8.8 \pm 0.1$. The G6P^{-2} species has 11 bounded hydrogen atoms and its oxidation to 6PDGL releases two hydrogen atoms. Therefore, the value $\bar{N}_H = 8.8$ suggests that most of the G6PDL species has a −2 charge in the studied pH range.

5. Conclusions

The determination of kinetic and thermodynamic parameters of the reaction catalyzed by G6PD from *L. mesenteroides* in phosphate buffer was possible using a spectrophotometric *in situ* method. The thermal instability was observed at 43 °C and can be compared with other works with G6PD from *S. cerevisiae* [4]. From kinetic and thermodynamic results, it is possible to say that the reaction is pH dependent due to the G6P and, probably, 6PDGL ionization, principally at pH < 7. The influence of the His-240 residue protonation [1] in G6PD was observed on the kinetic constants of the reaction. The effect of relative initial concentrations is important on transformed Gibbs energy of reaction values at pH >6. Apparently, the 6PDGL has a predominant −2 charge and its standard Gibbs energy of formation was calculated by employing the corresponding equations for biochemical reactions [8,9], this value is independent of the temperature (292.15 ≤ T/K ≤ 310.15) and the pH (5.4 ≤ pH ≤ 8.6).

Acknowledgments

The authors thank the Mexican Council of Science and Technology (Conacyt) for the financial support through the Project 58290. JSMC thanks Conacyt for her grant.

Appendix A. Supplementary data

Supplementary data associated with this article can be found, in the online version, at doi:10.1016/j.tca.2011.01.030.

References

[1] M.S. Cosgrove, S.N. Loh, J.H. Ha, H.R. Levy, Biochemistry 41 (2002) 6939–6945.
[2] C.E. Naylor, S. Gover, A.K. Basak, M.S. Cosgrove, H.R. Levy, M.J. Adams, Acta Crystallographica Section D 57 (2001) 635–648.
[3] M.S. Cosgrove, C. Naylor, S. Paludan, M.J. Adams, H.R. Levy, Biochemistry 37 (1998) 2759–2767.
[4] F.A. Hasmann, D.B. Gurpilhares, I.C. Roberto, A. Converti, A. Pessoa, Enzyme and Microbial Technology 40 (2007) 849–858.
[5] F.G. Rossi, M.Z. Ribeiro, A. Converti, M. Vitolo, A. Pessoa, Enzyme and Microbial Technology 32 (2003) 107–113.
[6] R.N. Goldberg, Y.B. Tewari, T.N. Bhat, Bioinformatics 20 (2004) 2874–2877.
[7] V. Vought, T. Ciccone, M.H. Davino, L. Fairbairn, Y. Lin, M.S. Cosgrove, M.J. Adams, H.R. Levy, Biochemistry 39 (2000) 15012–15021.
[8] R.A. Alberty, Pure and Applied Chemistry 66 (1994) 1641–1666.
[9] R.A. Alberty, Thermodynamics of Biochemical Reactions, Wiley, New Jersey, 2003.
[10] C. Olive, M.E. Geroch, H.R. Levy, The Journal of Biological Chemistry 246 (1971) 2047–2057.
[11] W.T. Lee, H.R. Levy, Protein Science 1 (1992) 329–334.
[12] M.L. Bianconi, Biophysical Chemistry 126 (2007) 59–64.
[13] A. Salis, D. Bilanicová, B.W. Ninham, M. Monduzzi, Journal of Physical Chemistry B 111 (2007) 1149–1156.
[14] H.J. Engel, W. Domschke, M. Alberti, G.F. Domagk, Biochimica et Biophysica Acta 191 (1969) 509–516.
[15] N.G. Brink, Acta Chemica Scandinavica 7 (1953) 1081–1089.
[16] M.L. Bianconi, The Journal of Biological Chemistry 278 (2003) 18709–18713.